

QQ-PLOT FOR SEQUENTIAL ORBIT DETERMINATION

James R Wright*

Abstract

Use of the Kalman measurement update theorem for sequential orbit determination incurs *the requirement*, from fundamental hypothesis, that post-fit measurement residual ratios have a standard normal distribution. When the residual sample size is small, comparison to the normal density curve is not useful because small-sample normal ensembles do not resemble the infinite-ensemble normal curve (bell curve). The quantile-quantile (QQ) plot with Royston-Michael acceptance boundaries for normal distributions is useful for small and large ensembles. Herein I demonstrate the application of QQ-Plots to simulated measurement residual ratios. On real data, QQ-Plots will be used to demonstrate, or deny, that *the requirement* is satisfied.

INTRODUCTION

Electronic measurements are used to estimate spacecraft orbit states, attitude states, clock states, and time-varying bias states due to measurement bias and force model bias. Herein I refer to post-fit measurement residual ratios (measurement residual/root-variance) derived from the use of a sequential filter-smoother algorithm for orbit determination. Electronic measurement sequences all have significant thermal noise components, and every thermal noise sequence has a *normal* distribution[2]. Measurement residuals are a composition of measurement thermal noise and random modeling errors. Every measurement residual ratio is a standard normal variate when serially correlated residual components are removed by optimal state estimation.

Measurement residual ratio histograms are compared to the standard normal density function¹ $N(0, 1)$ in Figures 1 and 2. This comparison enables one to identify undesired characteristics (measurement bias, histogram² peakedness, or histogram flatness) when ensemble size is large. When ensemble size is small the histogram comparison is not useful. Quantitative acceptance boundaries are not available for histograms, large or small.

We consider here the application of QQ-Plots and their acceptance boundaries to measurement residual ratios derived from electronic measurements. An hypothesis for both the QQ-Plot test, and for the Kalman measurement update theorem, is that the post-fit measurement residual ratios be white; i.e., independent and identically distributed. Post fit measurement residual ratios due to *optimal* state estimation are white[3][4]. Thus *optimality* can be supported, or denied, with a whiteness test³.

Given the use of simulated *perfect* models for spacecraft acceleration, attitude, and measurements, and the use of simulated measurement data with simulated thermal noise, then post-fit measurement residual ratios should be standard normal $N(0, 1)$ variates. Inspection of the QQ-Plot on post-fit measurement residual ratios enables immediate quantitative validation of these simulated models.

*ODTK Architect, Analytical Graphics, Inc., 220 Valley Creek Blvd, Exton, PA, 19341

¹Notation $N(\mu, \sigma^2)$ refers to a normal distribution with mean μ and variance σ^2 . Notation $N(0, 1)$ refers to a *standard* normal distribution because it has mean 0 and variance 1.

²My use of words *peakedness* and *flatness* does not refer to *kurtosis* (defined in [9]).

³An appropriate whiteness test was presented by John Seago[8] and David Vallado.

Given the use of *imperfect* models for spacecraft acceleration, attitude, and electronic measurements, and given real electronic measurements whose measurement thermal noise is not masked (e.g., by truncation of the measurement word length), then post-fit measurement residual ratios are used in a QQ-Plot to identify existence of imperfections in the models used. This enables (in part) the development and validation of appropriate model corrections. For validation of sufficiently designed models, it is necessary that post-fit measurement residual ratios have the standard normal $N(0, 1)$ distribution, and this is easily verified by application of the QQ-Plot. Inspection of the QQ-Plot enables validation for normal distribution, identification of non-normal distribution, and quantifies additive bias, density function peakedness, and density function flatness.

The fundamental hypothesis for the Kalman filter[3][4], adapted for use by ODTK⁴, requires that ODTK measurement residuals and state estimate modeling error corrections have normal distributions⁵. Since each measurement residual is mapped *linearly* to the state estimate correction matrix using the Kalman gain matrix, then the state estimate error correction matrix belongs to a normal distribution if the measurement residual belongs to a normal distribution. Thus if each measurement residual ratio is shown to belong to a standard normal distribution by application of a QQ-Plot, then we have simultaneously demonstrated that each state estimate error correction matrix belongs to a normal distribution. The QQ-Plot is used to demonstrate, or deny, that the fundamental hypothesis for the Kalman filter is satisfied.

1 Histograms

Measurement residuals are a composition of measurement thermal noise and random modeling errors – inclusive of force modeling errors and measurement bias. Denote measurement thermal noise (white noise) root variance by σ_{WN} , and denote Gauss-Markov sequence measurement bias root variance by σ_{GM} . Values for σ_{WN} and σ_{GM} are required ODTK filter inputs for each measurement type on each sensor. Each measurement residual ratio is defined with measurement residual in the numerator and measurement residual root-variance in the denominator. When the measurement residual variance input value is significantly too small, filter performance can become unstable, eventually leading to filter divergence. When the measurement residual variance input value is significantly too large, state estimate corrections are too large and optimal accuracy performance is degraded.

To correct a peaked histogram, reduce the size of the measurement residual ratio denominator to increase the histogram frequency width. To correct a flattened histogram, increase the size of the measurement residual ratio denominator to reduce the histogram frequency width.

Figures 1 and 2 present real-data examples that compare a peaked measurement residual ratio histogram with its corrected histogram. Table 1 presents operational values associated with the peaked histogram of Figure 1, and corrected values associated with the corrected histogram of Figure 2. Note that root variances σ_{WN} and σ_{GM} were reduced to correct the peaked histogram.

	C bias (m)	σ_{GM} bias (m)	σ_{WN} (m)
peaked	563	100	7.62
corrected	800	30	1.00

Table 1: Residual Ratio Histogram Correction

⁴Orbit determination tool kit (ODTK) is a software capability, licensed and offered by Analytical Graphics, Inc (AGI).

⁵Kalman used Sherman’s Theorem as theoretical foundation for the Kalman filter, but he restricted his use of the class of Sherman distributions to the normal distribution in order to obtain a computationally tractable algorithm.

QQ-PLOT

Motivation

Given any two sets of data X and Y , each with n elements x_j and y_j for $j \in \{1, 2, \dots, n\}$, we want to determine graphically if sets X and Y are the same, or if they are "close" to each other. Order each set smallest to largest. Suppose set X is known. If $y_j = x_j$ for⁶ each j , then the graph $q(x_j) = y_j = x_j$ lies on a diagonal straight line (Figure 3), and set Y is known because $Y = X$.

For random sets of data X and Y , where $Y \neq X$, but Y is sufficiently close to X , and the distribution function for X is known, then the distribution function for Y is also known. Choose set X to be an ordered set of n standard Normal variates. Then if set Y of ordered elements is sufficiently close to set X , then set Y is also a set of n standard Normal variates.

Definition

Abscissa x

Quantiles on the abscissa are normal variates, derived by inversion of the standard normal $N(0, 1)$ cumulative distribution function (CDF) $F(x)$. $F(x)$ is defined by Equation 1, using dummy variable η notation, and is graphed in Figure 4.

$$F(x) = \frac{1}{\sqrt{2\pi}} \int_{-\infty}^x \exp(-\eta^2/2) d\eta \quad (1)$$

$F(x)$, on the ordinate of Figure 4, is partitioned here uniformly on the interval $[0, 1]$ in increments of 0.1. Notice that $x = 0$ for $F(x) = 0.5$. That is $F(x) = 0.5$ implies

$$x = F^{-1}(0.5) = 0$$

Similarly for $F(x) = 0.69146246$ ⁷

$$x = F^{-1}(0.69146246) = 0.5$$

Generally

$$F^{-1}(F(x)) = x \quad (2)$$

Example Given ten uniformly centered values of $F(x)$, then values for $x = F^{-1}(F(x))$ were calculated and are displayed in Table 2. The ten values of x thus calculated, symmetric about the origin, are the x-axis quantiles for our first QQ-Plot.

Ordinate y for Simulation

Draw n values randomly from an $N(0, 1)$ standard normal distribution to simulate post-fit measurement residual ratios, and order them smallest to largest to define the y-axis quantiles.

Ordinate y for Real Measurement Residual Ratios

Given n measurement residual ratios, order them smallest to largest, to define n real-data y-axis quantiles.

⁶Elements x_j and y_j for the ideal case are of course not random.

⁷See Abramowitz[1] page 966.

$F(x)$	x
0.05	-1.6448536
0.15	-1.0364334
0.25	-0.67448975
0.35	-0.38532047
0.45	-0.12566135
0.55	+0.12566135
0.65	+0.38532047
0.75	+0.67448975
0.85	+1.0364334
0.95	+1.6448536

Table 2: Abscissa Quantiles

x-axis Quantiles	y-axis Quantiles
-1.6448536	-1.1805311
-1.0364334	-0.34795186
-0.67448975	-0.30266471
-0.38532047	-0.27558085
-0.12566135	-0.16322556
+0.12566135	+0.035624810
+0.38532047	+0.067902558
+0.67448975	+0.234433610
+1.0364334	+0.82798437
+1.6448536	+1.2870826

Table 3: QQ Table

QQ-Plot

Each pair of quantiles (x, y) defines a dot to be plotted in the plane. Connect the dots to construct a QQ-Plot.

Example Figure 5 presents the QQ-Plot (a jagged red line within the smooth blue envelope) derived from Table 3.

ROYSTON-MICHAEL ACCEPTANCE BOUNDARIES

The two smooth blue curves of Figure 5 are Royston-Michael[7] acceptance boundaries for the QQ-Plot. Royston's application of Michael's[5] theoretical development addresses only normal distributions. Royston suggests validity of sample size N for $7 \leq N \leq 1000$, based on fairly exhaustive testing, and validity for $1000 \leq N \leq 2000$, based on minimum testing. The sample size for Figure 5 is ten, and thus falls at the lower end of sample size validity range.

Table 4 associates α (Alpha) with the normal σ (Sigma) interval for the scalar standard normal distribution $N(0, 1)$.

Royston's suggested range validity for α is $50\% \leq \alpha \leq 99.5\%$. Test significance is defined by the $(100 - \alpha)$ per-cent level. Figure 5 uses $\alpha = 99.5\%$, thus test significance for Figure 5 is 0.5%.

The Royston acceptance boundary construction algorithm is a specialization of Michael's[5] results to normal distributions. Michael used results due to Noe[6]. From the title of Noe's paper one sees that Royston's algorithm for QQ-Plot acceptance boundaries derives from theory that reaches back to Kolmogorov and Smirnov (KS) and the KS test statistic.

Alpha	Sigma
68.2689492137%	± 1
95.4499736104%	± 2
99.7300203937%	± 3
99.9936657616%	± 4
99.9999426697%	± 5
99.999998027%	± 6

Table 4: Associate Alpha with Sigma

Boundaries

The lower Royston-Michael boundary y_{iL} , for $i \in \{1, 2, \dots, n\}$, is defined (Royston[7], page 154, Section 2.2)

$$y_{iL} = \bar{y} + \sqrt{v}F^{-1}(\sin^2 d_i) \quad (3)$$

where \bar{y} is the sample mean on test quantiles, v is the sample variance about the sample mean on test quantiles, and d_i is called a critical point. Each critical point d_i is calculated by an empirically derived algorithm given by Royston (page 154, Section 2.3).

The upper Royston-Michael boundary y_{iU} , for $i \in \{1, 2, \dots, n\}$, is defined

$$y_{iU} = \bar{y} - \sqrt{v}F^{-1}(\sin^2 d_{n-i+1}) \quad (4)$$

Graphically, the upper boundary y_{iU} is symmetric with the lower boundary y_{iL} in that the d_{n-i+1} are the d_i in inverted order⁸.

Undefined d_i

Critical point d_i is undefined if the calculation given for d_i is negative or zero (Royston, page 154, Section 2.2). Most of the examples presented herein have undefined points at the beginning of the lower bound sequence in d_i , and symmetrically at the end of the upper bound sequence in d_i . This must be accounted for when graphing the lower and upper boundaries. Inspection of Figure 5 reveals one blank space at the beginning (left side) of the lower boundary (associate first corner in the QQ line), and one blank space at the end (right side) of the upper boundary (associate last corner in the QQ line).

QQ-PLOT COMPARISONS BETWEEN A NORMAL DISTRIBUTION AND A NON-NORMAL SHERMAN DISTRIBUTION

Distinction between a Normal distribution and a non-Normal Sherman distribution, for a particular α level, is achieved if the QQ-Plot does cross either boundary line. Distinction, for a particular α level, is not achieved if the QQ-Plot does not cross either boundary line.

The QQ-Plot capability to distinguish between Normal and non-Normal Sherman distributions is dependent on sample size when sample size is small. With Figure 14, sample size 200 and $\alpha = 90.0\%$, the QQ-Plot *does* distinguish between a Normal and a non-Normal Sherman distribution. With Figure 15, sample size 100 and $\alpha = 90.0\%$, the QQ-Plot *does not* distinguish between a Normal and a non-Normal Sherman distribution. See the subsection *Sherman Distributions* below for definition of the particular non-Normal Sherman distribution used.

⁸For C^{++} indexing with k rather than i , where $k \in \{0, 1, 2, \dots, n-1\}$, replace y_{iU} with y_{kU} and $(\sin^2 d_{n-i+1})$ with $(\sin^2 d_{n-k-1})$ in Equation 4.

TEST QUANTILE DISTRIBUTIONS DISTINGUISHED BY QQ-PLOT

Normal

Simulations

Figures 5 through 11 present QQ-Plots within acceptance boundaries. Normal $N(0, 1)$ distributions are thereby indicated.

Figures 7 and 8 have sample size 1000, and have $\alpha = 99.5\%$. But Figure 7 presents an unbiased QQ-Plot, whereas the QQ-Plot of Figure 8 has a positive bias of 1σ , created by adding 1σ to simulated normal $N(0, 1)$ test quantiles. The bias is quantified explicitly by inspection of the QQ-Plot at zero on the abscissa.

Figures 9 and 10 quantify flatness and peakedness of associated histograms by angular rotations of the QQ-Plot away from the diagonal with slope $m = 1$. Measure the slope $m > 0$ from a QQ-Plot, then calculate the variance σ^2

$$\sigma^2 = 1/m^2 \tag{5}$$

where $m = 1$ implies $\sigma^2 = 1$. Figure 9 is flattened with slope $m = 2 = 1/\sqrt{0.25}$ with $\sigma = 1/2$, and Figure 10 is peaked with slope $m = 1/2 = 1/\sqrt{4}$ with $\sigma = 2$.

Real Data

Let Δy_k denote real measurement residuals produced by orbit determination at time t_k , for $k \in \{1, 2, \dots, n\}$, and let $\Delta \mathbf{y}$ denote a random variable with values Δy_k . Approximately

$$E\{\Delta \mathbf{y}\} = 0 \tag{6}$$

Define the unknown true variance σ^2 on $\Delta \mathbf{y}$

$$\sigma^2 = E\{(\Delta \mathbf{y})^2\} \tag{7}$$

Let $\hat{\sigma}^2$ denote an estimate of σ^2 , input by the operator to the orbit determination filter algorithm. Construct a histogram of ratios $\Delta y_k/\hat{\sigma}$, and overlay it with a graph of $N(0, 1)$. If $\hat{\sigma} > \sigma$, then the histogram is peaked relative to $N(0, 1)$, the filter gain magnitudes are too large, filter correction magnitudes are too large, the autonomous filter editor does not reject as many outliers as expected, and the mean-squared state error is not minimized. But if $\hat{\sigma} < \sigma$, then the histogram is flattened relative to $N(0, 1)$, the filter gain magnitudes are too small, filter correction magnitudes are too small, an excessive number of measurements are rejected by the autonomous filter editor, and the mean-squared state error is not minimized. An example of a peaked histogram is presented in Figure 1 where $\hat{\sigma} > \sigma$. Figure 2 was obtained after adjustment of $\hat{\sigma}$ to achieve $\hat{\sigma} \approx \sigma$. Both histograms are (approximately) normal. Think of Figure 1 as a scaled version of Figure 2. This is a manual iterative procedure. Automation can be achieved with the QQ-Plot. Calculate the

- QQ-Plot on Δy_k for $k \in \{1, 2, \dots, n\}$
- QQ-Plot slope m
- variance $\sigma = 1/m$ (Equation 5)

Non-Normal Simulations

Figure 12 responds to having replaced one of the original normal $N(0, 1)$ quantiles near the origin with a 4σ outlier, namely 4, prior to calculating boundaries. Figure 12, with $\alpha = 90\%$, shows the QQ-Plot crossing acceptance boundaries. The test quantiles are rejected as normal $N(0, 1)$ test quantiles.

Sherman Distributions

By definition, a Sherman probability distribution function $S(\mathbf{x})$ is symmetric about its mean $\bar{\mathbf{x}}$, and is convex for all $\mathbf{x} \leq \bar{\mathbf{x}}$. Normal distributions are Sherman distributions, but there are an infinite number of Sherman distributions that are not normal distributions. Figure 17 was derived from the non-Normal Sherman distribution function $S_1(x)$

$$S_1(x) = \begin{cases} 0 & \text{if } x < -3 \\ \frac{1}{4}(2 + x - x^3/27) & \text{if } -3 \leq x \leq 3 \\ 1 & \text{if } x > 3 \end{cases} \quad (8)$$

and Figure 18 was derived from the associated non-Normal Sherman density function $s_1(x)$

$$s_1(x) = \begin{cases} 0 & \text{if } x < -3 \\ \frac{1}{4}(1 - x^2/9) & \text{if } -3 \leq x \leq 3 \\ 0 & \text{if } x > 3 \end{cases} \quad (9)$$

The associated Sherman test quantiles of Figure 13 with sample size 1000, and Figure 14 with sample size 200, derived from $S_1(x)$, are distinguished as non-Normal distributions by their QQ-Plots. The associated Sherman test quantiles of Figure 15 with sample size 100, and Figure 14 with sample size 10, derived from $S_1(x)$, are *not* distinguished as non-Normal distributions by their QQ-Plots.

SAMPLE-SIZE DEPENDENCE

QQ-Plots with acceptance boundaries are presented for sample sizes of 10, 50, 1000, and 100000 (this last case is not supported or denied by Royston). Boundaries are observed to "close-in" as sample size increases.

MEASUREMENT RESIDUAL RATIOS

Significant thermal noise $w(t)$ exists as a time-varying component in all electronic spacecraft tracking measurements. Thermal noise has a normal distribution $N(0, \sigma_w^2(t))$ with mean 0 and variance $\sigma_w^2(t)$, where

$$\sigma_w^2(t) = E\{w^2(t)\}$$

Form the ratio

$$R(t) = \frac{w(t)}{\sigma_w(t)}$$

and notice that $R(t)$ has a standard normal $N(0, 1)$ distribution.

$$E\{R(t)\} = 0$$

$$E\{R^2(t)\} = 1$$

ACKNOWLEDGEMENT

John Seago (AGI) suggested the use of the QQ-Plot with Royston acceptance boundaries to validate, or deny validation of, ODTK measurement residual ratios. John provided the Royston and Michael papers, and was helpful in the validation of the Royston boundary algorithm.

References

- [1] Abramowitz, Milton, Stegun, Irene A., *Handbook of Mathematical Functions*, NBS, 1964, 10th printing 1972
- [2] Davenport, Wilbur B., Root, William L., *An Introduction to the Theory of Random Signals and Noise*, McGraw-Hill, New York, 1958, Section 9-4 Thermal Noise, page 185
- [3] Kalman, R. E., *New Methods in Wiener Filtering Theory*, Proceedings of the First Symposium on Engineering Applications of Random Function Theory and Probability, edited by J. L. Bogdanoff and F. Kozin, John Wiley & Sons, New York, 1963
- [4] Meditch, J. S., *Stochastic Optimal Linear Estimation and Control*, McGraw-Hill, New York, 1969.
- [5] Michael, John R., *The Stabilized Probability Plot*, Biometrika, 70, 1., pp 11-17, 1983
- [6] Noe, Marc, *The Calculation of Distributions of Two-Sided Kolmogorov-Smirnov Type Statistics*, The Annals of Mathematical Statistics, Vol. 43, No. 1, 58-64, 1972
- [7] Royston, Patrick, *Graphical Detection of Non-Normality by Using Michael's Statistic*, Appl. Statist., 42, No. 1, pp 153-158, 1993
- [8] Seago, J.H., D.A. Vallado (2010), *Goodness-of-Fit Tests for Sequential Orbit Determination*, Paper AAS 10-149, from Mortari, D. et al. (eds), Space Flight Mechanics 2010 - Advances in the Astronautical Sciences, Vol. 136, Part I, Proceedings of the 13th AAS/AIAA Space Flight Mechanics Meeting, San Diego, California, February 14-17, 2010, pp. 749-768
- [9] Stuart, Alan, Ord, J. Keith, *Kendall's Advanced Theory of Statistics*, Vol. 1, Hodder Arnold, Sixth Edition, 1994, page 109

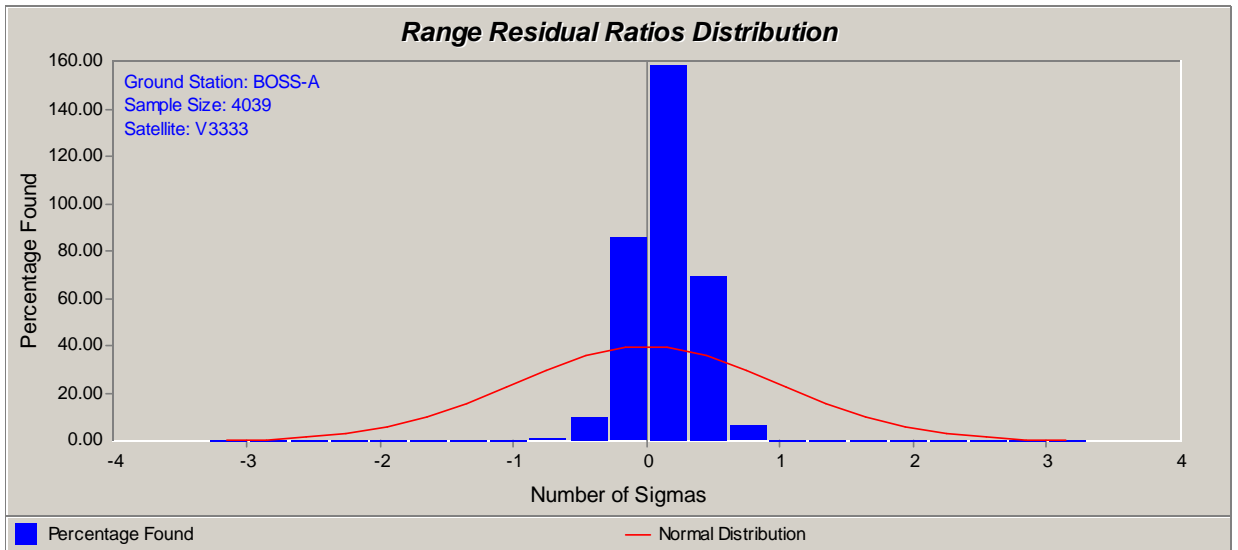


Figure 1: Peaked Histogram of Real Range Residual Ratios *Before* Calibration

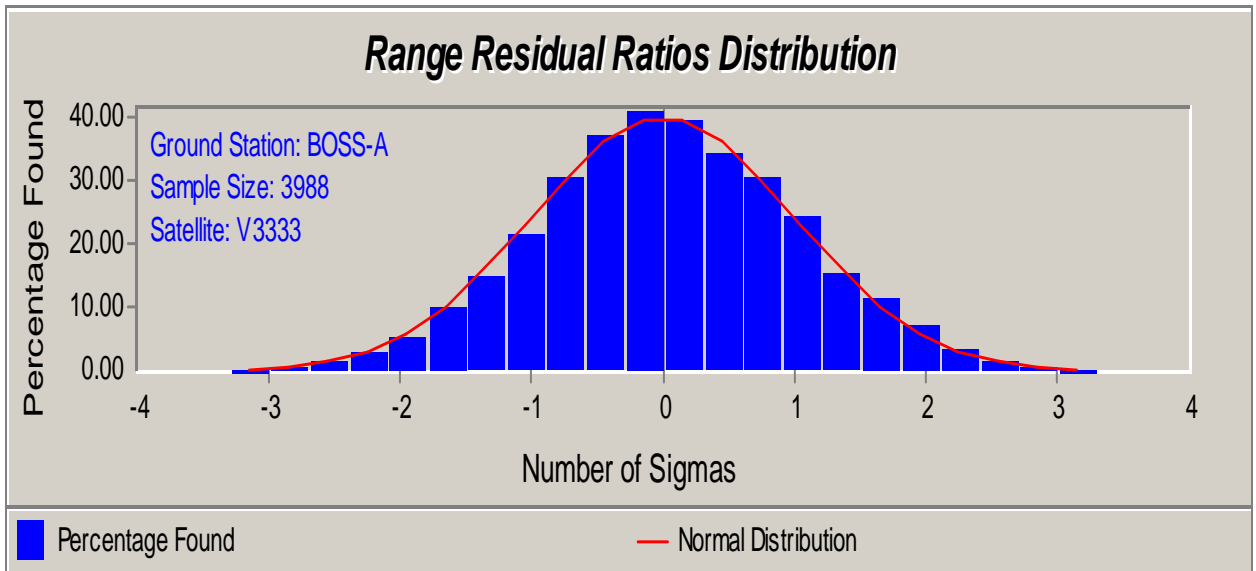


Figure 2: Normal $N(0, 1)$ Histogram of Real Range Residual Ratios *After* Calibration

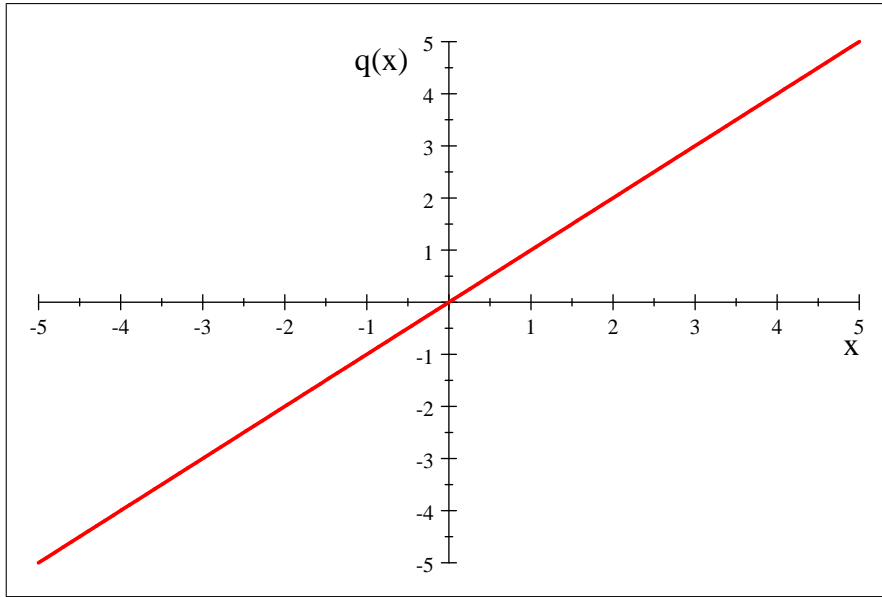


Figure 3: Ideal QQ-Plot

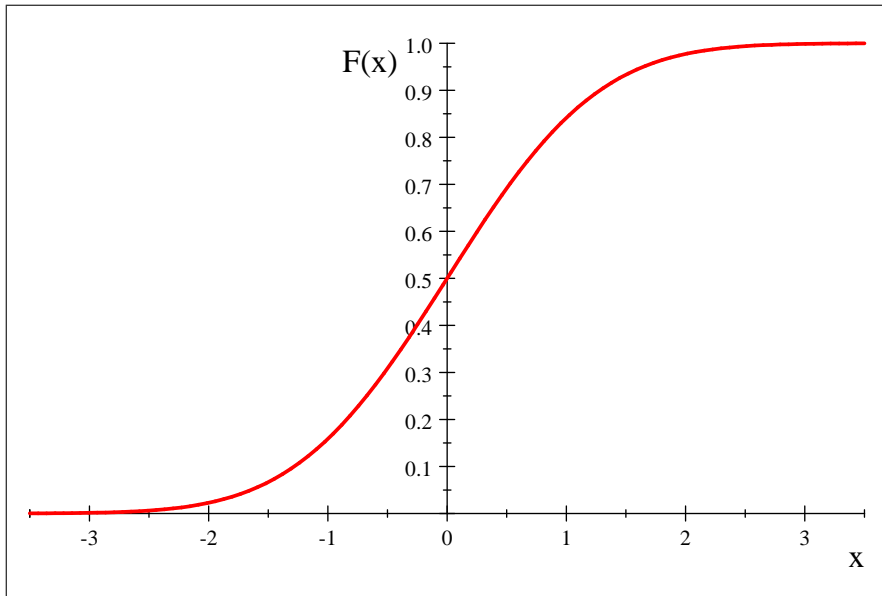


Figure 4: Standard Normal Cumulative Distribution Function

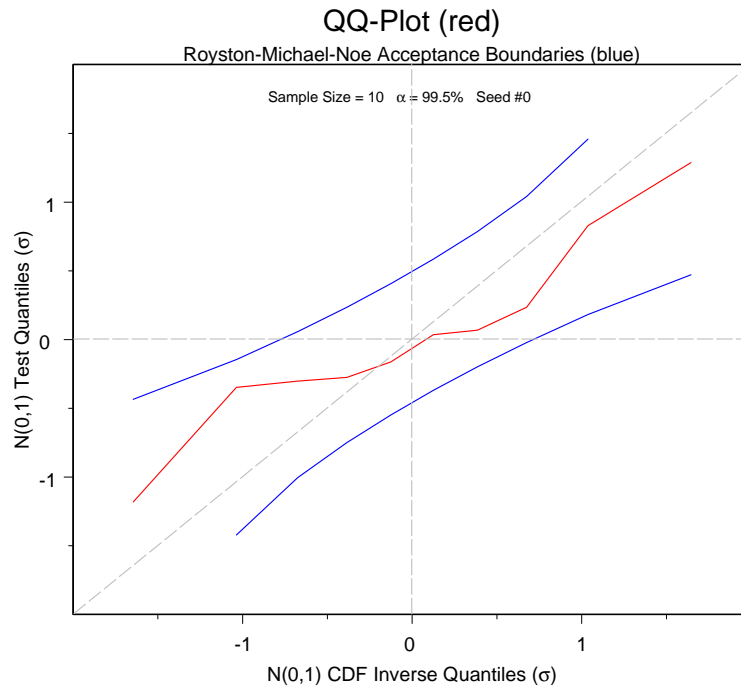


Figure 5: A Perfect QQ-Plot of Sample Size 10

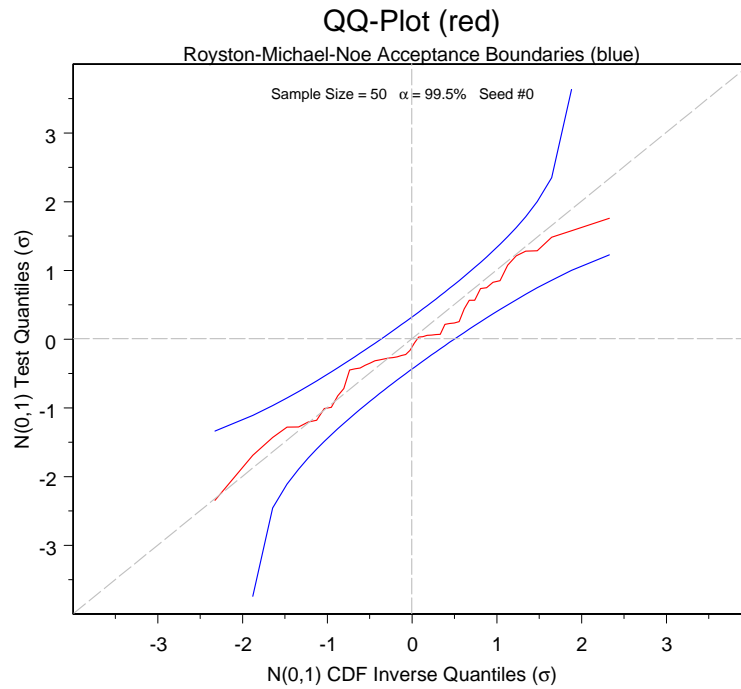


Figure 6: Sample Size 50 Alpha 99.5%

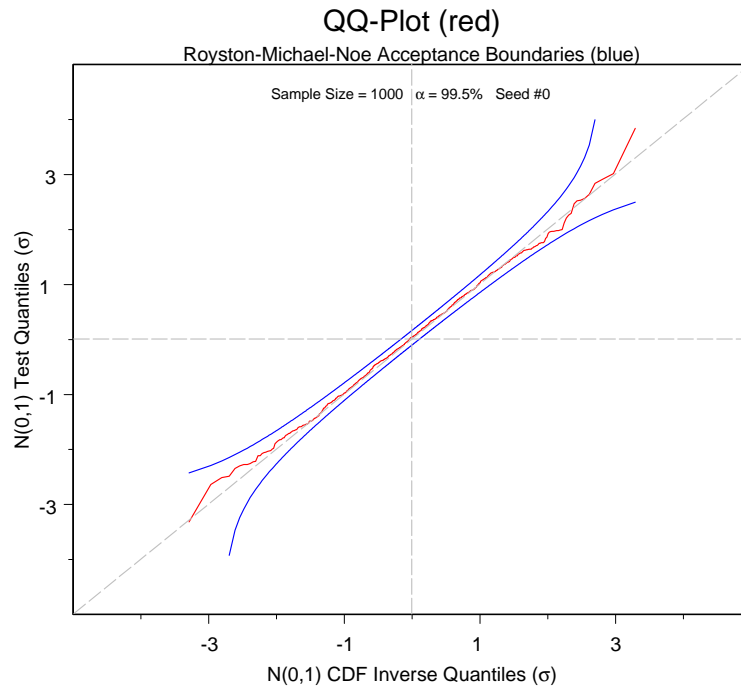


Figure 7: Sample Size 1000 Alpha 90.5%

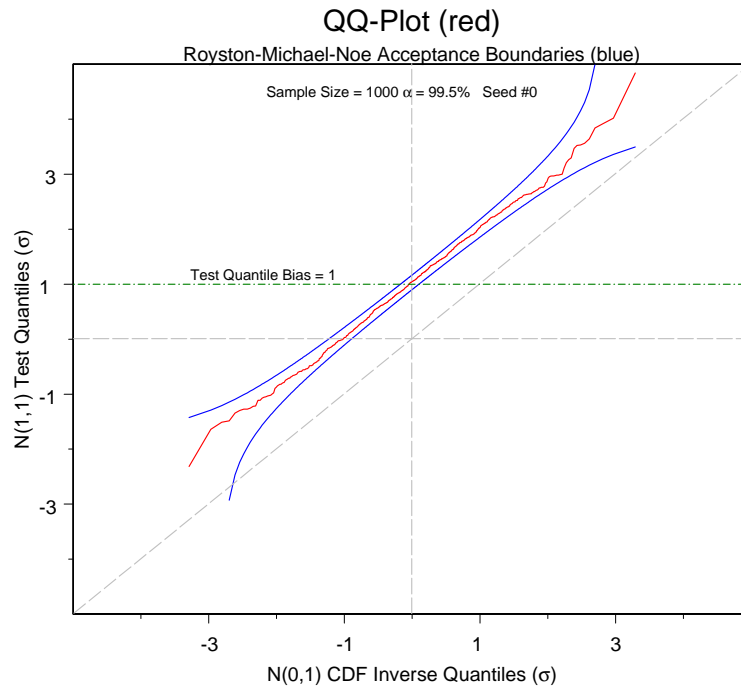


Figure 8: Test Quantiles Biased 1 Sigma

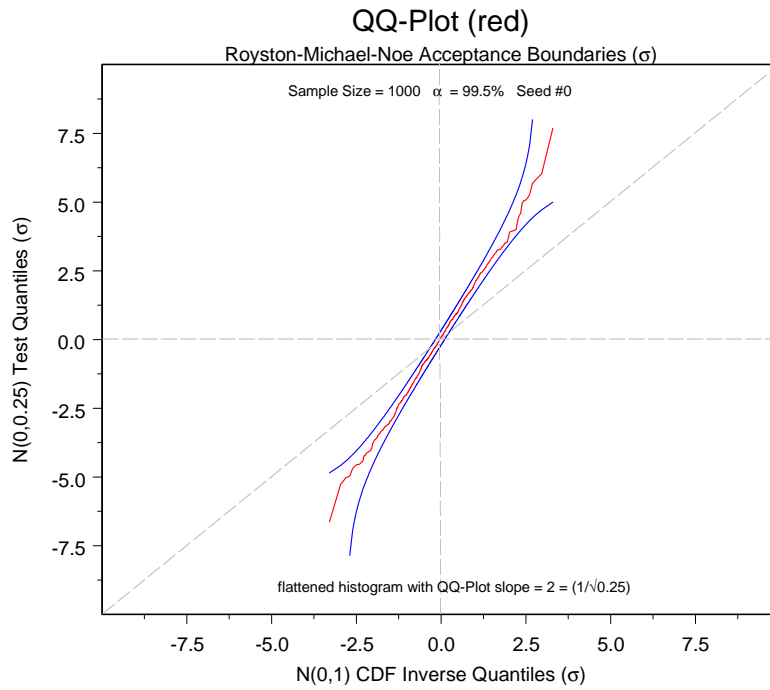


Figure 9: Slope > 1 Implies Flattened Histogram

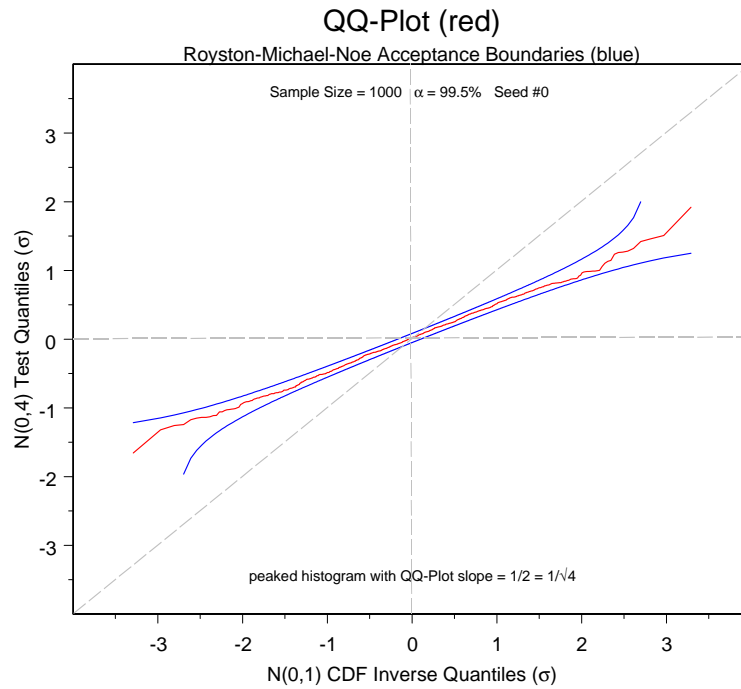


Figure 10: Slope < 1 Implies Peaked Histogram

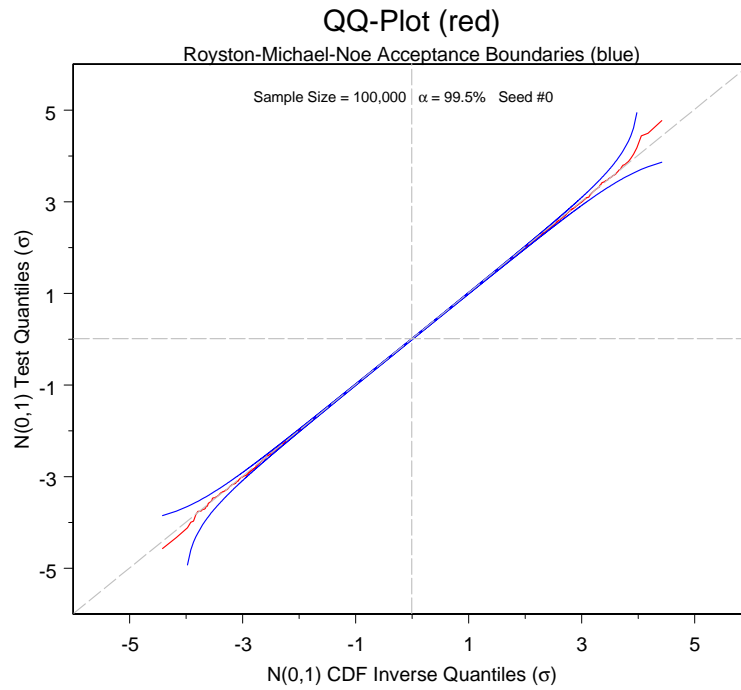


Figure 11: Sample Size 100000 Alpha 99.5%

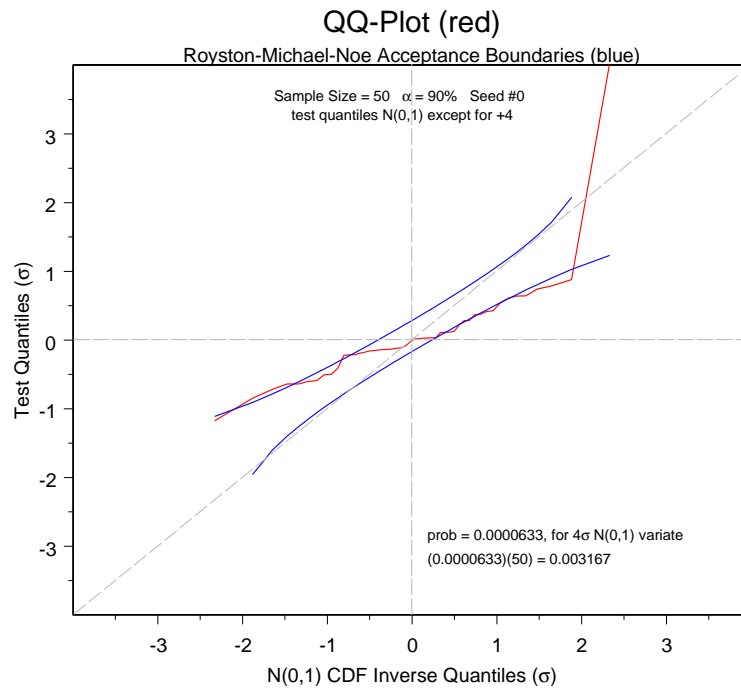


Figure 12: Test Quantiles: Forty-Nine N(0,1) Variates & One with Value 4

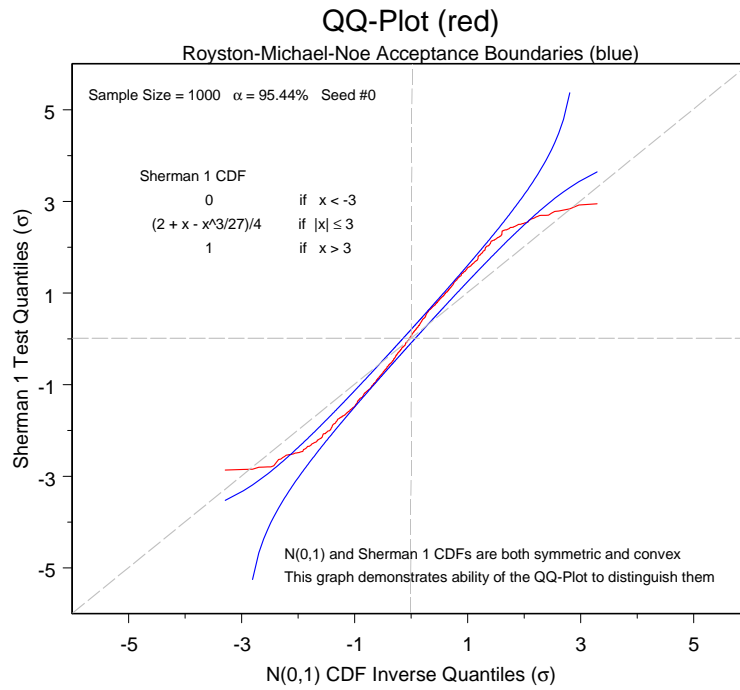


Figure 13: Sample Size 1000 Does Distinguish Sherman 1 from $N(0,1)$

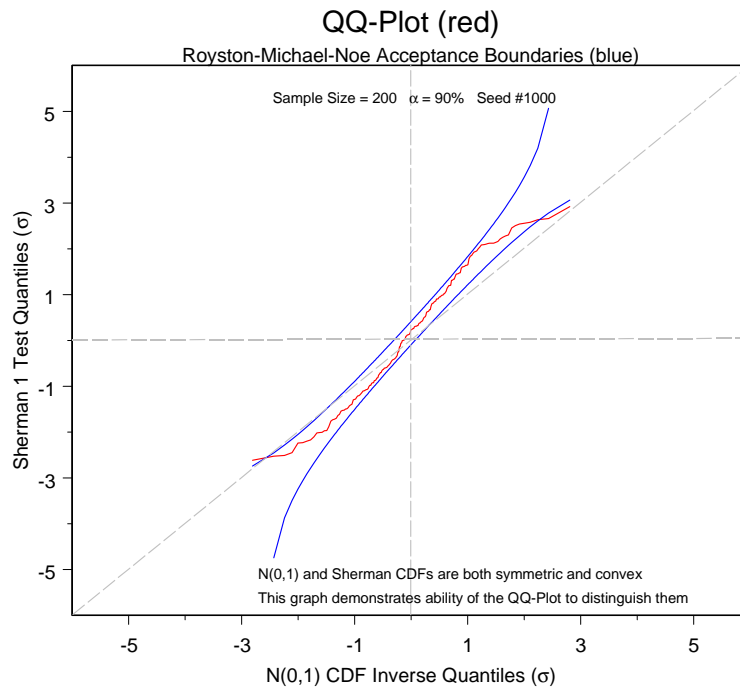


Figure 14: Sample Size 200 Does Distinguish Sherman 1 from $N(0,1)$

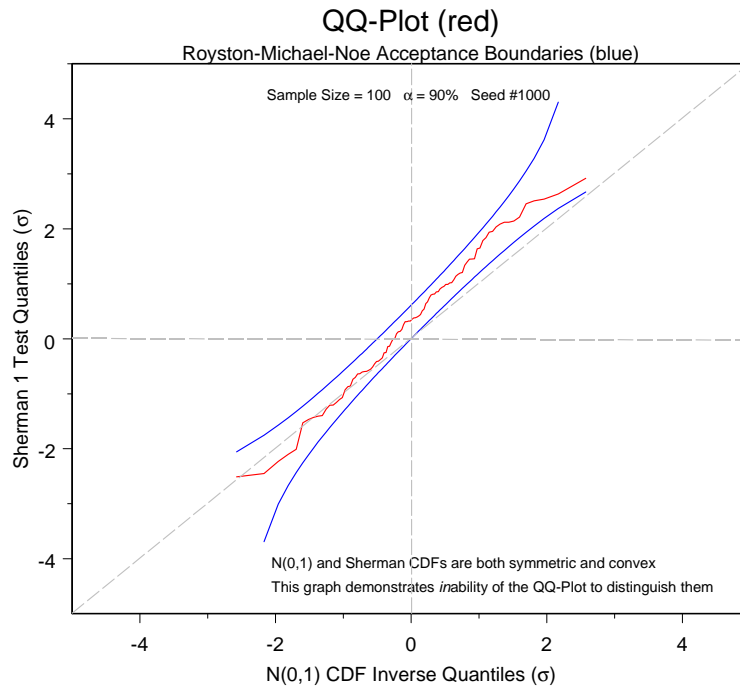


Figure 15: Sample Size 100 Does Not Distinguish Sherman 1 from $N(0,1)$

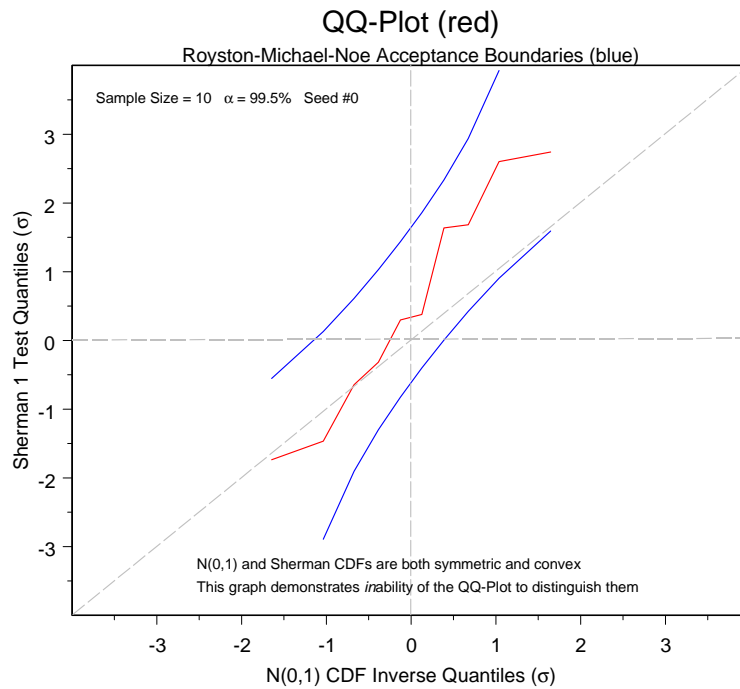


Figure 16: Sample Size 10 Does Not Distinguish Sherman 1 from $N(0,1)$

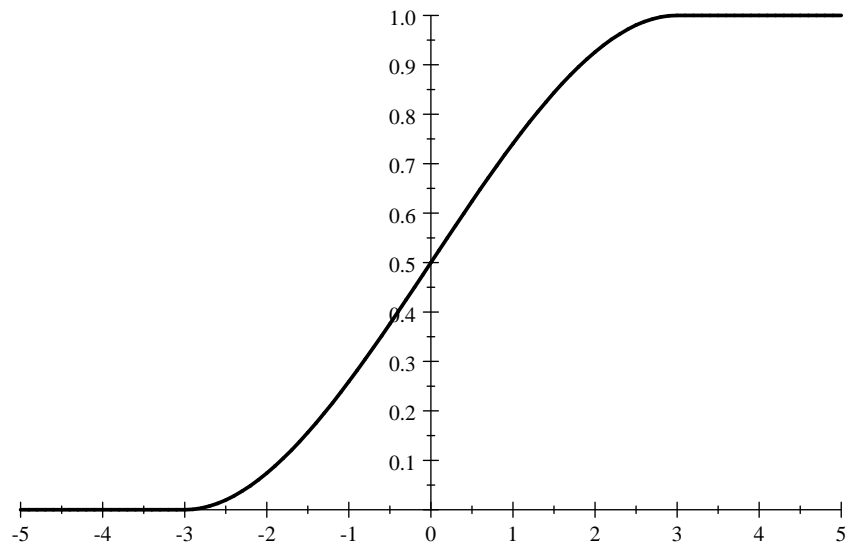


Figure 17: Sherman Probability Distribution Function $S_1(x)$

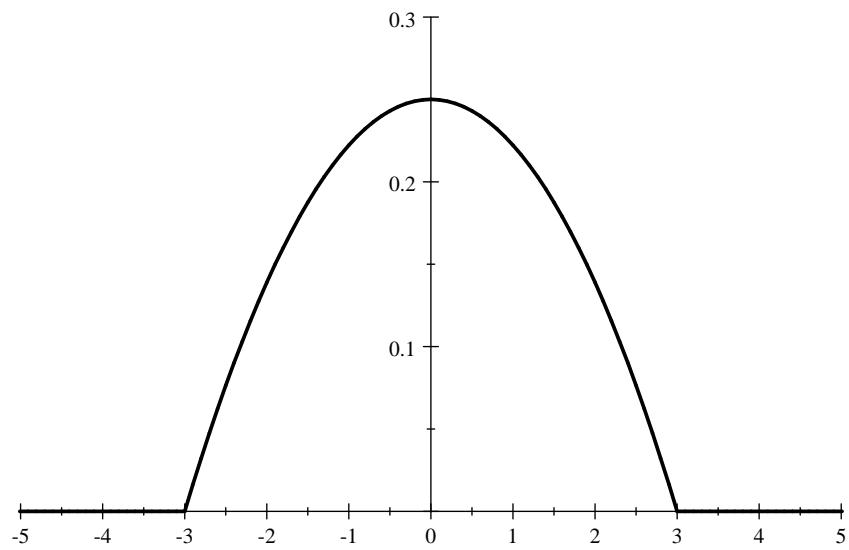


Figure 18: Sherman Probability Density Function $s_1(x)$